The Journal of Experimental Biology 204, 1783–1794 (2001)
Printed in Great Britain © The Company of Biologists Limited 2001
JEB3338

A MAXI Cl^- CHANNEL IN CULTURED PAVEMENT CELLS FROM THE GILLS OF THE FRESHWATER RAINBOW TROUT *ONCORHYNCHUS MYKISS*

M. J. O'DONNELL*, S. P. KELLY, C. A. NURSE AND C. M. WOOD

Department of Biology, McMaster University, 1280 Main Street West, Hamilton, Ontario, Canada L8S 4K1

*e-mail: odonnell@mcmaster.ca

Accepted 22 February; published on WWW 23 April 2001

Summary

Primary cultures of pavement cells from the gills of a freshwater fish, the rainbow trout *Oncorhynchus mykiss*, have been studied for the first time using the patch-clamp technique. Gigaohm seals were obtained in approximately 95 % of cells studied, and channel activity was evident in a high proportion (>90 %). A large-conductance Cl^- channel was evident in 6 % of cell-attached and in 31 % of inside-out patches. Single-channel conductance in inside-out patches was 372 pS, and current/voltage relationships were linear over the range −60 to +60 mV. The channel was activated by patch excision, and activation was often associated with polarization of the patch. The mean number of channels per patch was 1.9, and there were several subconductance states. The relationship between channel activity (NP_o) and voltage was in the form of an inverted U, and channel activity was highest between 0 and +20 mV. Large-conductance Cl^- channels showed a progressive time-dependent reduction in current in response to sustained polarization to voltages outside the range −20 mV to +20 mV. Permeability ratios (P) of Cl^- to other anions were P_{HCO_3}/P_{Cl}=0.81, P_{SO_4}/P_{Cl}=0.31 and $P_{isethionate}/P_{Cl}$=0.53. The channel was blocked by Zn^{2+}, SITS, DIDS and diphenylamine carboxylate. This is the first description of a large-conductance Cl^- channel in gill cells from freshwater or marine species. Possible functions of the channel are discussed.

Key words: patch-clamp, 'maxi' Cl^- channel, Zn^{2+}, SITS, DIDS, gill, freshwater teleost, rainbow trout, *Oncorhynchus mykiss*.

Introduction

Current models of ion transport by the gills of teleost fish have proposed that Na^+ is actively transported by the pavement (respiratory) cells, whereas the transport of Ca^{2+} and Cl^- is accomplished by the mitochondria-rich cells, also known as chloride cells (Goss et al., 1995; Perry, 1997). This division of function has been challenged, however, by several recent studies using primary cultures of pavement cells. A detailed immunofluorescence study has revealed the presence of vacuolar-type proton pumps and amiloride-sensitive epithelial Na^+ channels in the apical membranes of the mitochondria-rich cells of the freshwater rainbow trout *Oncorhynchus mykiss* (Wilson et al., 2000). Active uptake of Cl^- by cultured pavement cells derived from the gills of *O. mykiss* has been demonstrated (Wood et al., 1998; Fletcher et al., 2000). Active secretion of Cl^- has been observed in primary cultures of pavement cells from the gills of the sea bass *Dicentrarchus labrax* (Avella and Ehrenfeld, 1997; Duranton et al., 1997).

A small-conductance Cl^- channel that may be involved in Cl^- secretion has been revealed by patch-clamp studies of the apical membrane of cultured pavement cells of the sea bass (Duranton et al., 1997). A conductance of 8 pS was observed in cell-attached patches. The channel is active at all membrane holding potentials in inside-out patches, but the open probability (P_o) decreases when the membrane is hyperpolarized and increases strongly with depolarization. Channel activity is increased by the application of protein kinase A and ATP. The proposed model of transepithelial Cl^- secretion in primary cultures of sea bass pavement cells postulates that Cl^- entry across the basolateral membrane is mediated by $Na^+/K^+/2Cl^-$ cotransport and Cl^-/HCO_3^- exchange. Cl^- is accumulated above equilibrium levels, then moves down its electrochemical gradient through cyclic-AMP-stimulated apical Cl^- channels (Duranton et al., 1997).

An 8 pS Cl^- channel has also been identified in primary cultures of the mitochondria-rich cells from the opercular epithelium of the euryhaline marine killifish *Fundulus heteroclitus* (Marshall et al., 1995). Stimulation with cyclic AMP increased the proportion of cell-attached patches that contained the channel and also increased the incidence of patches with multiple channels. The channel usually became inactive after excision.

These results of patch-clamp analysis of the ion channels of cultured pavement cells or mitochondria-rich cells from marine species suggest that comparable studies of cell cultures derived from the gills of freshwater species would aid our

understanding of the transport mechanisms involved in ion uptake by the gills of freshwater teleosts. This paper describes the application of patch-clamp techniques to the study of ion transport by primary cultures of pavement cells of the rainbow trout *Oncorhynchus mykiss*. We report the presence and characteristics of a large-conductance Cl^- channel in the apical membrane. Its very large single-channel conductance and voltage-dependent gating properties give this channel a characteristic signature.

Materials and methods

Cell culture

Procedures for the preparation and culture of gill pavement cells were based on those developed previously (Wood and Pärt, 1997) with slight modifications. Gill tissue was obtained from a stock of rainbow trout *Oncorhynchus mykiss* (Walbaum) (150–200 g) held in dechlorinated running Hamilton tapwater (composition: $[Na^+]$=0.55 mmol l^{-1}, $[Cl^-]$=0.70 mmol l^{-1}, $[Ca^{2+}]$=1.00 mmol l^{-1}, $[Mg^{2+}]$=0.15 mmol l^{-1}, $[K^+]$=0.05 mmol l^{-1}, pH 7.8–8.0) at seasonal temperatures (13–17 °C). All procedures for the isolation and culture of gill cells were conducted in a laminar-flow hood using sterile techniques. Isolation of gill cells from branchial tissues was achieved by tryptic digestion (Gibco BRL Life Technologies, 0.05 % trypsin in phosphate-buffered saline, PBS, with 5.5 mmol l^{-1} EDTA). After two consecutive 20 min cycles of tryptic digestion, the cells were resuspended in culture medium (Leibovitz's L-15 supplemented with 2 mmol l^{-1} glutamine, 5–6 % foetal bovine serum, FBS, 100 i.u. ml^{-1} penicillin, 100 μg ml^{-1} streptomycin and 200 μg ml^{-1} gentamycin) and seeded into 25 cm^2 culture flasks (Falcon) at a density of 520×10^3 cells cm^{-2}. The flasks were held in an air atmosphere at 18 °C. Non-adherent cells were removed from the culture flasks by changing the medium 24 and 96 h after initial seeding. From 96 h onwards, newly added medium was free of antibiotics. Previous studies have shown that the cells survive well when antibiotics are eliminated after 3–4 days in culture (Fletcher et al., 2000). Antibiotics were therefore removed from the medium to avoid any non-specific xenobiotic effects on cultured cells. After a further 48–72 h of culture, cells were harvested by the removal and replacement of medium with trypsin solution (see above). Flasks were monitored for cell detachment under a phase-contrast microscope, and trypsination was terminated by adding suspended cells to a stop solution (10 % FBS in PBS, pH 7.7). Cells were resuspended in medium and seeded onto sterile 35 mm diameter Petri dishes at a density of approximately 50×10^3 cells ml^{-1} in 250–300 μl drops. After incubation overnight at 18 °C, the medium was changed, and 2–2.5 ml of fresh medium was added to the dishes. Thereafter, the medium was changed every 48 h. Cells were used for experiments after 2–6 days in culture.

Patch-clamp techniques

We used both the cell-attached (on-cell) and inside-out configurations of the patch-clamp technique. Micropipettes were pulled from 1.5 mm external diameter filamented glass capillary tubing (AM Systems Inc., Carslborg, WA, USA) on a Flaming-Brown pipette puller (model P97). After fire polishing, micropipettes had tip resistances of 2–7 MΩ when filled with standard recording solution.

Patch-clamp recordings were made with an EPC9 computer-controlled patch-clamp amplifier (Heka Elektronik GmbH Lambrecht/Pfalz, Germany) and version 8.4 of the Pulse/PulseFit or PulseTools software. All data were recorded at 2.9–10 kHz using integral three-pole and four-pole Bessel filters. Traces for the figures were subsequently filtered using a digital non-lagging Gaussian filter (i.e. software filter) with the −3 dB cut-off frequency set to 300–500 Hz. Additional data analysis and graphing were performed with Igor 3.15 (WaveMetrics, Lake Oswego, OR, USA). Junction potentials were corrected using JPCalc (Barry, 1994). Outward currents and depolarizing voltages are displayed as positive deflections in current and voltage recordings.

Solutions

For most experiments, the patch pipette was filled with an extracellular fluid hereafter referred to as '150 NaCl solution' and containing (in mmol l^{-1}): 150 NaCl, 0.1 $CaCl_2$, 1 $MgCl_2$, 10 glucose and 10 Hepes at pH 7.2. The bath solution was usually identical to the pipette solution for the initial characterization the channel. All experiments were conducted at 22 °C. The intracellular pH of pavement cells at 19 °C is 7.4 (Wood and Pärt, 2000) and, since most experiments were conducted on inside-out patches, the pH of 7.2 for the bath solution was chosen to approximate the intracellular pH at the slightly higher temperature used in this study. Internal bathing solutions used in studies of ion channels in trout red blood cells were also adjusted to pH 7.2 (Egée et al., 1997b).

In some experiments, the pipette was filled with a solution that contained (in mmol l^{-1}): 145 KCl, 1.4 $CaCl_2$, 1.2 $MgCl_2$, 10 glucose and 10 Hepes at pH 7.2. The bathing solution contained either the same solution (for on-cell recordings) or 145 mmol l^{-1} KCl, 5 mmol l^{-1} EGTA, 0.29 mmol l^{-1} $CaCl_2$, 1.2 mmol l^{-1} $MgCl_2$, 10 mmol l^{-1} glucose and 10 mmol l^{-1} Hepes at pH 7.2. The 'free' Ca^{2+} activities of the latter two solutions, calculated using the Max Chelator algorithm (http://www.stanford.edu/ cpatton/webmaxc2.htm), were 10^{-3} mol l^{-1} and 10^{-8} mol l^{-1}, respectively. The two solutions are hereafter referred to as '145 KCl, pCa 3' and '145 KCl, pCa 8', respectively.

To determine the ion selectivity of the channel, the cytoplasmic surface of inside-out patches was perfused with one or more of five different solutions (see Stea and Nurse, 1989): A, B, C, D or E. All five solutions were at pH 7.2 and contained (in mmol l^{-1}) 0.1 $CaCl_2$, 1 $MgCl_2$, 10 glucose and 10 Hepes. In addition, solution A contained 75 mmol l^{-1} NaCl, solution B contained 75 mmol l^{-1} NaCl and 75 mmol l^{-1} choline chloride, solution C contained 75 mmol l^{-1} NaCl and 75 mmol l^{-1} sodium isethionate, solution D contained 75 mmol l^{-1} NaCl and 75 mmol l^{-1} $NaHCO_3$ and solution E contained 75 mmol l^{-1} NaCl and 37.5 mmol l^{-1} Na_2SO_4.

Channel activity

Channel activity (NP_o, where N is the number of available channels and P_o is open probability) was calculated in two ways. In the first, mean open-channel current (I) during 20 sweeps for 1 s each was divided by the single-channel current i ($NP_o=I/i$; see Markwardt et al., 1997; Al-Nakkash and Hwang, 1999; Kameyama et al., 1997). In the second method, channel activity was measured from voltage ramps (as described by Carl and Sanders, 1990). The latter method is useful for patches containing more than one channel and permits measurement of NP_o over a large range of voltages. The averaged current from 15–20 ramp protocols was divided by the single-channel current at each potential calculated from the reversal potential and the slope conductance.

Selectivity

Single-channel conductance in media of different ionic composition was calculated from the slope of leak-corrected current–voltage (I/V) plots derived from recordings of single-channel currents measured during voltage ramps. The ramps were usually from −40 mV to +40 mV or from −60 mV to +60 mV. The Cl^- selectivity of the channel was determined from experiments in which Na^+ and Cl^- were the predominant ions present and were reduced in concentration in the bathing solution. The permeability ratio of Na^+ to Cl^- was calculated using the Goldman–Hodgkin–Katz equation, as follows:

$$E_{rev} = \boldsymbol{R}T/F\ln\frac{[Cl^-]_b + (P_{Na}/P_{Cl})[Na^+]_p}{[Cl^-]_p + (P_{Na}/P_{Cl})[Na^+]_b}, \quad (1)$$

where E_{rev} is the reversal potential obtained from the single-channel I/V plot, $\boldsymbol{R}$, T and F have their usual meanings, P is permeability, b refers to the external (bathing) solution and p refers to the pipette solution. The permeability ratio of other anions (A^-) relative to Cl^- (P_A/P_{Cl}) was determined by substituting the calculated value of P_{Na}/P_{Cl} into the Goldman–Hodgkin–Katz equation, as follows:

$$E_{rev} = \boldsymbol{R}T/F\ln\frac{[Cl^-]_b + r(P_A/P_{Cl})[A^-]_b + (P_{Na}/P_{Cl})[Na^+]_p}{[Cl^-]_p + r(P_A/P_{Cl})[A^-]_p + (P_{Na}/P_{Cl})[Na^+]_b}, \quad (2)$$

where r is the ratio of the valences of the anion to that of Cl^-.

Channel blockers

The pharmacological properties of the anion channel were examined by superfusing the cytoplasmic surface of inside-out patches with putative Cl^- channel blockers dissolved in the 150 NaCl bathing solution. All channel blockers were obtained from Sigma; they included 10 mmol l^{-1} anthracene-9-carboxylic acid (9-AC), 0.2–1 mmol l^{-1} 4,4′-diisothiocyanatostilbene-2,2′-disulphonic acid (DIDS), 1 mmol l^{-1} diphenylamine carboxylate (DPC), 1 mmol l^{-1} 4-acetamido-4′-isothiocyanatostilbene-2,2′-disulphonic acid (SITS; Sigma) and 1 mmol l^{-1} Zn^{2+} (as the chloride salt). All drugs were dissolved directly in the control bathing solution except 9-AC, which was dissolved in dimethyl sulphoxide (DMSO) so that the final concentration of DMSO was less than 1 %.

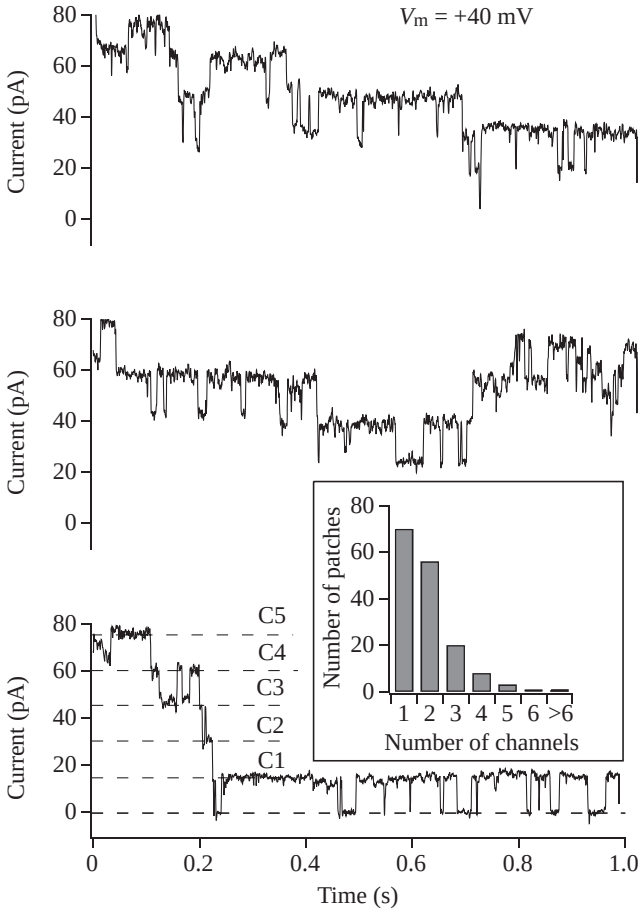

Fig. 1. The top two traces show recordings of five large-conductance Cl^- channels in a single inside-out patch in 150 NaCl solution (see Materials and methods). V_m, membrane potential. Dashed lines in the bottom panel show current levels corresponding to the opening of one (C1) to five (C5) channels. The inset histogram shows the frequency of occurrence of patches containing multiple channels (N=159 patches).

Results

Gigaohm seals were obtained in approximately 95 % of the attempts at seal formation. For 568 successful seals, typical seal resistance was 1–20 GΩ, and the typical duration of seal integrity was more than 20 min in cell-attached patches and more than 30 min in inside-out patches. Loss of seal integrity was usually associated with polarization to membrane voltages outside the range −60 mV to +60 mV, although some seals became unstable and were lost if polarization to voltages outside the range −20 mV to +20 mV was maintained for more than a few seconds. Channel activity was observed in 92 % of patches (523/568). Small- and intermediate-conductance channels were not studied in detail. The characteristics of a large-conductance (>350 pS) ‘maxi’ channel are described below. This channel was observed in 28 % of all patches (159/568). Maxi channels were observed in 6 % of cell-attached patches (36/568) and in 31 % of inside-out patches (159/508).

Channel density

A high proportion of the 159 patches with maxi channels

had more than one channel per patch (Fig. 1). The mean number of channels per patch was 1.93±0.10.

Channel conductance

Channel conductance was calculated from leak-corrected single-channel *I/V* plots derived from recordings made during voltage ramps from −40 to +40 mV or from −60 to +60 mV (Fig. 2). Conductance was linear (r^2>0.99) over these ranges with 150 NaCl as both the internal and external solutions. The mean values of channel conductance calculated from the *I/V* plots were 361±11 pS (*N*=16 cells) for cell-attached patches and 372±5 pS (*N*=68 cells; means ± S.E.M.) for inside-out patches. There were at least two subconductance states (Fig. 3) at approximately one-third and two-thirds of the full conductance: 137±17 pS (*N*=4) and 261±8 pS (*N*=19) (means ± S.E.M.). It is unlikely that these current levels were due to openings or closings of other smaller-conductance channels in the patch because they were not observed in patches that did not contain the maxi anion channel. Moreover, subconductance states were most common in channels during the early stages of activation, as described below. Fully activated channels were more commonly found to have transitions between the fully open and fully closed states, with only infrequent openings to the subconductance levels.

Channel activation after excision

Although maxi channel activity was found in only 6% of cell-attached patches, patch excision was often associated with the induction of channel activity. For 138 patches that showed maxi channel activity in inside-out patches and for which recordings were obtained in both the cell-attached and inside-out modes, only 18 showed maxi channel activity before excision. For the other 120 patches (87%), channel activity appeared only after excision. In most cases, this activation was not immediate, but developed over several minutes following excision and appeared to be accelerated by polarization to voltages outside the range −30 mV to +30 mV. In recordings at both a single voltage (Fig. 4) and in voltage ramps (Fig. 5), activity began as noisy events of short duration and/or at a subconductance level and then developed into longer openings of the highest conductance state. After full openings had been induced, channels did not return to the flickery transition mode while bathed in the standard solution.

Recordings from inside-out patches showed that the maxi channel was not Ca^{2+}-dependent. Channel activity and conductance were unaffected when the 145 KCl, pCa 3 solution was replaced with the 145 KCl, pCa 8 solution (*N*=16 patches).

Voltage-dependent relaxation of maxi channels

Maxi channels showed a progressive time-dependent reduction in current in response to sustained polarization to

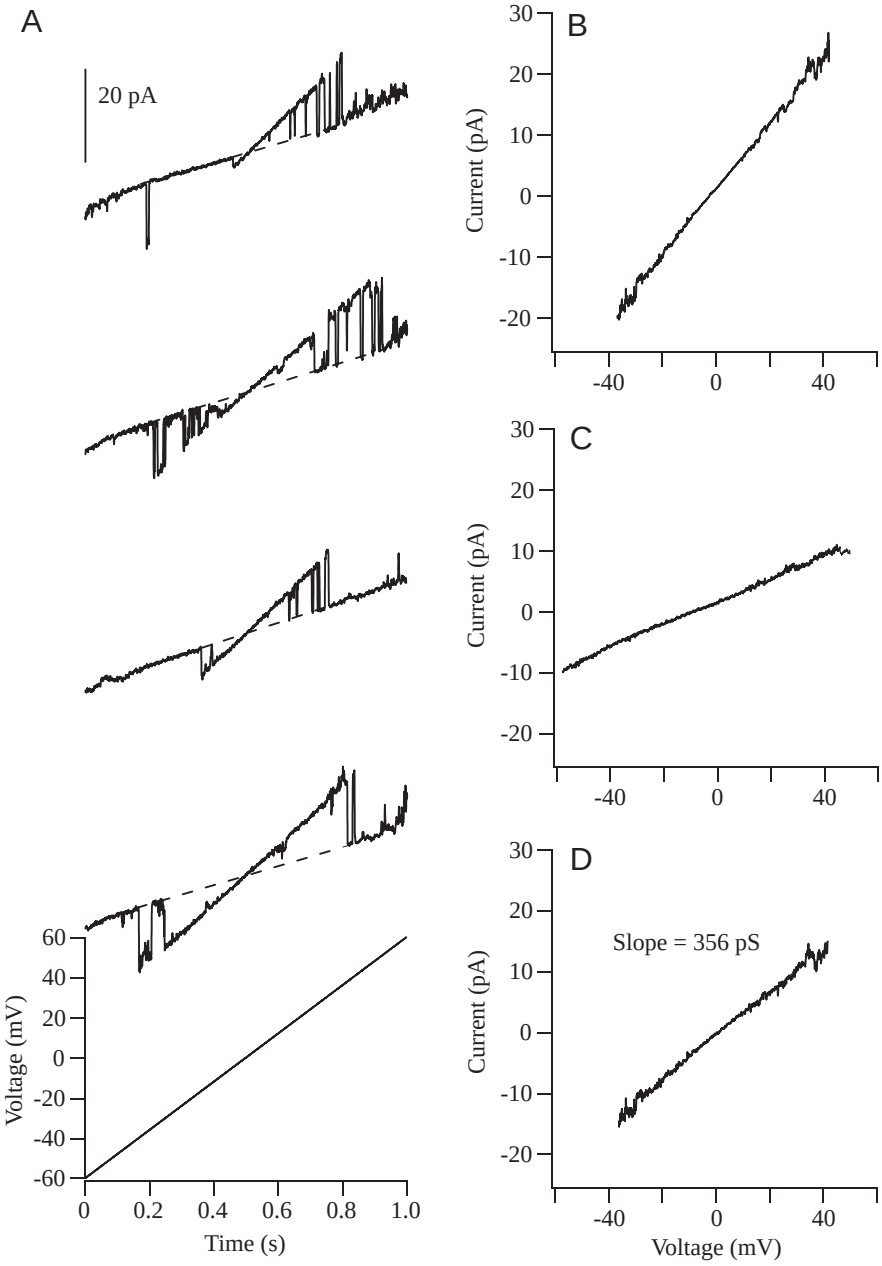

Fig. 2. Single-channel current/voltage (*I/V*) relationships. All recordings were from a single inside-out patch that contained only one large-conductance Cl^- channel. (A) Four current recordings in response to the voltage ramp protocol indicated at the bottom of the panel. The dashed lines correspond to the current levels for the closed state of the channel. B–D were obtained from conditional averaging of 20 recordings from the same patch. (B) Mean open-channel current, (C) mean leak current (i.e. closed-channel current) and (D) leak-corrected single-channel current (values in B minus values in C).

voltages outside the range –20 mV to +20 mV (Fig. 6A). The reduced channel activity at voltages outside this range was reflected in time-dependent closing of the channel. For these experiments, 1 s voltage jumps from 0 mV to positive or negative voltages were applied with a 200 ms recovery period between successive sweeps. Additional representative recordings at a membrane voltage of +40 mV are shown in Fig. 6B for a patch containing three channels. Channels closed in a stepwise fashion during the 1 s voltage jump from 0 to +40 mV. The activity of channels that closed during pulses to voltages outside the range –40 mV to +40 mV recovered if the membrane potential was returned to the range –20 mV to +20 mV. The kinetics of channel closing was estimated from ensemble averages of 15–20 individual current responses to the same test pulse (Fig. 6C,D). The mean current was well-described by a single exponential, and the associated relaxation time constant (τ) was inversely related to membrane voltage.

Voltage-dependence of channel activity (NP_o*)*

Channels typically were nearly always open at voltages from approximately –20 to approximately +20 mV. Although activity declined at voltages outside this range, the value of NP_o was typically greater than zero (Fig. 7) even at the extremes (–50 mV to +60 mV). Currents were not recorded at larger voltages because seal integrity was often lost if the patch was polarized for more than a few tens of milliseconds to voltages outside the range –60 mV to +60 mV.

The voltage-dependence of channel activity was also assessed using currents recorded during voltage ramp (Fig. 8). By dividing the mean leak-corrected current recorded during the ramp (Fig. 8A) by the corresponding single-channel current (Fig. 8B), a continuous plot of NP_o over the voltage range was obtained (Fig. 8C,D).

The inverted U-shape of the plot of NP_o as a function of membrane voltage was evident in recordings for individual patches and in the mean values plotted at intervals for ramps from –60 mV to +60 mV (Fig. 8D) or –40 mV to +40 mV (not shown; N=17 patches). A broad peak of channel activity was observed at membrane potentials of +10 mV to +20 mV. The relationship between NP_o and voltage (V) was well described by the sum of one rising and one falling Boltzmann distribution (Fig. 8D).

The absence of maxi channel activity in cell-attached patches was not due to the presence of a cell-negative membrane potential. For 55 cell-attached patches for which no maxi channel activity was seen when membrane voltage was ramped from –100 mV to +100 mV, channel activity appeared after excision. Assuming a typical cell membrane potential of less than –100 mV, the membrane potential across the patch would have reached 0 mV or positive voltages by the end of the ramp. Similarly, for 13 cell-attached patches in which the cells were depolarized by exposure to 145 KCl, pCa 3 solution, there was no channel activity prior to patch excision.

Channel selectivity

Preliminary ion-substitution experiments indicated that the maxi channel was more permeable to anions than to cations. A change from symmetrical internal and external solutions to a situation in which the concentration of KCl (Fig. 9) or NaCl (not shown) was reduced caused the single-channel reversal potential to shift towards the Cl^- equilibrium potential. Using single-channel I/V plots from inside-out patches subjected to voltage ramps, the value of P_{Na}/P_{Cl} calculated from the reversal potentials (see Materials and methods) was 0.11±0.09 (N=5) and P_K/P_{Cl} was 0.08±0.03 (N=3; means ± S.E.M.; P is permeability). The ability of the channel to pass other anions (bicarbonate, isethionate, sulphate) was determined by calculating their permeabilities relative to that of Cl^- using the modified Goldman–Hodgkin–Katz equation and substituting the estimated ratio for P_{Na}/P_{Cl} of 0.11. The calculated mean permeability ratios of the three other anions tested were P_{HCO_3}/P_{Cl}=0.81±0.11 (N=3), $P_{SO_{34}}/P_{Cl}$=0.31±0.04 (N=5) and $P_{isethionate}/P_{Cl}$=0.53±0.03

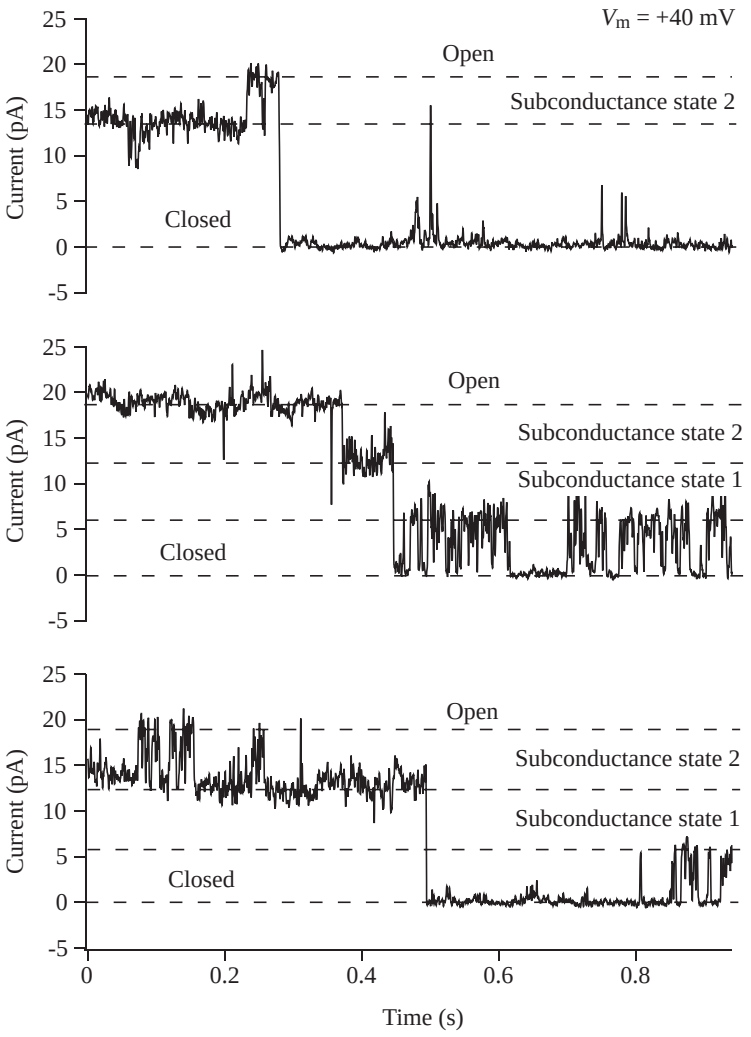

Fig. 3. Subconductance states for a single large-conductance Cl^- channel polarized to +40 mV. The dashed lines in the three recordings from an inside-out patch correspond to the current levels for the closed state or to openings to subconductance or fully open states. V_m, membrane potential.

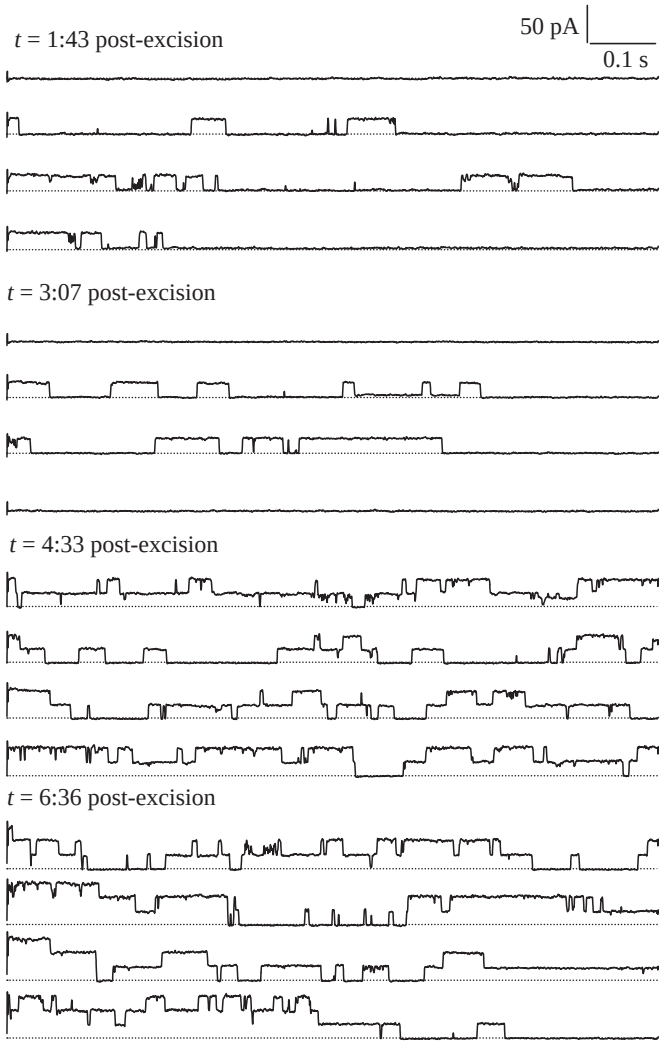

Fig. 4. Channel activation after excision. Current recordings from an inside-out patch at a membrane potential of +20 mV at the times indicated (min:s) after channel excision. No channel activity was noted in the same patch prior to excision. The zero current level is indicated by the dotted line in each recording.

(N=7; means ± S.E.M.). The permeability sequence was therefore $Cl^- > HCO_3^- >$ isethionate $> SO_4^{2-}$.

Effects of blockers of anion transport

The effects of putative blockers of Cl^- transport on the maxi channel were assessed in inside-out patches polarized to +20 mV. Drugs were applied to the external solution and, therefore, to the cytoplasmic side of the membrane. We did not study the effects of blockers applied in the pipette to the outside of the patch because of the very low frequency of occurrence of maxi channels in cell-attached patches. Application of 1 mmol l^{-1} Zn^{2+} to inside-out patches reduced channel current by 76±11 % (N=7; mean ± S.E.M.) below the control value, and blockade of the channel by Zn^{2+} was partly reversible (Fig. 10). The stilbene derivatives DIDS and SITS produced a nearly complete block of the maxi Cl^- channel. DIDS (0.2 mmol l^{-1}; Fig. 11) and SITS (1 mmol l^{-1}; Fig. 12) reduced channel current by 95±6 % (N=3) and 92±5 % (N=4; means ± S.E.M.), respectively, relative to the control value. Blockade by SITS was partly reversible, whereas block by DIDS was not reversed even by washing the patch with control external solution for more than 10 min. A flickery type of blockade was apparent in the early stages of channel blockade by 0.2 mmol l^{-1} DIDS. Channels opened only in bursts of very rapid flickering between open and closed states, as in the recordings after 4 min in the presence of DIDS (Fig. 11). The flickery blockade was followed by permanent inactivation (after 6–7 min in DIDS; Fig. 11).

Application of 1 mmol l^{-1} diphenylamine carboxylate (DPC) produced a nearly complete (>94 %) and irreversible block of the large-conductance anion channel (N=3 patches; data not shown). 9-Anthracene carboxylic acid (9-AC) at 10 mmol l^{-1} had no effect on single-channel currents (N=2).

Discussion

This paper reports the first application of the patch-clamp technique to pavement cells derived from the gills of a freshwater fish. Previous studies of cultured cells from marine fish, including pavement cells from the gills of sea bass *Dicentrarchus labrax* (Duranton et al., 1997) and the operculum of *Fundulus heteroclitus* (Marshall et al., 1995), support the presence of Cl^- channels of much smaller conductance (8 pS). Our results indicate the presence of a large-conductance Cl^- channel in pavement cells derived from

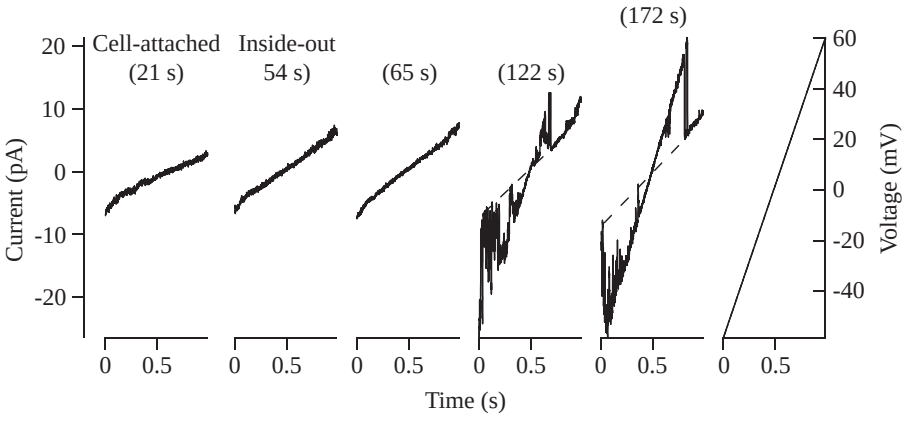

Fig. 5. Channel activation after excision in response to voltage ramps from –60 mV to +60 mV. The time course of the voltage ramp is shown in the right-hand panel. Membrane voltage was returned to 0 mV for 200 ms at the end of each ramp. Currents were recorded in the cell-attached mode (left-most recording) and in inside-out patches at the times indicated after patch formation. The dashed lines correspond to the current levels for the closed state of the channel. The patch was excised 30 s after patch formation.

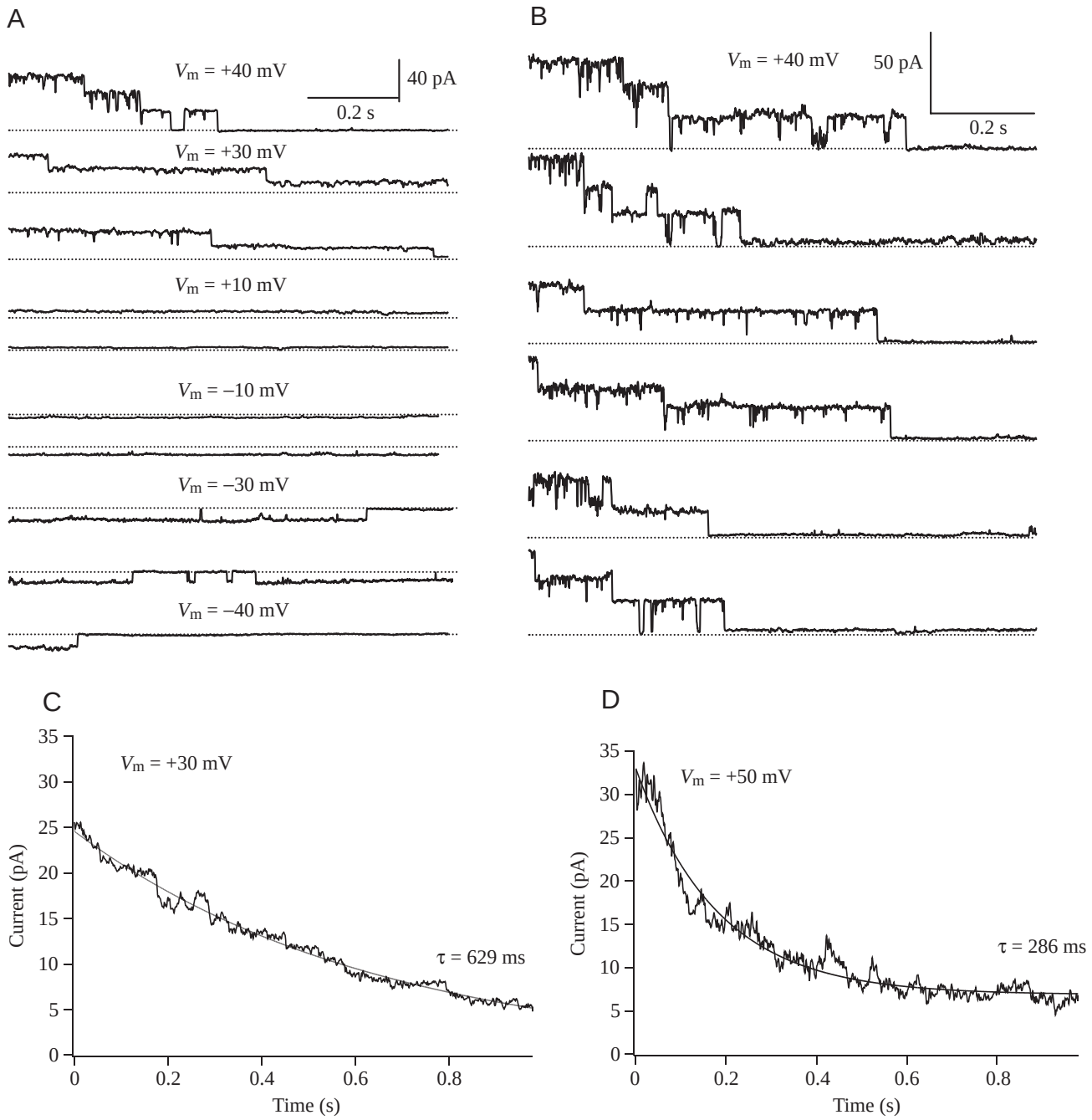

Fig. 6. (A) Voltage-dependent inactivation of large-conductance Cl^- channels. Currents were recorded from an inside-out patch polarized to the voltages (V_m) indicated. The patch contained at least three channels, evident in the top panel. The dotted line in each recording indicates the zero current level. Note that the channels close after a relatively short period of polarization to +40 or –40 mV. (B) Currents recorded from the same patch polarized to +40 mV, showing the progressive reduction in channel opening during successive sweeps. The patch voltage was returned to 0 mV for 200 ms between each sweep. Note that the channels were not inactivated, since each sweep starts with channels open for the early stages of polarization to +40 mV. (C,D) Ensemble average of current relaxations in response to 20 consecutive test pulses to +30 mV (C) or +50 mV (D). The time course of the current relaxation was fitted with a single exponential function (smooth lines) with the indicated time constant (τ), at which point the current had decayed by (1–1/e) or 63 %.

the gills of the freshwater trout. The channel is activated by patch excision, and activation is accelerated by polarization to voltages outside the range –30 mV to +30 mV. This channel shows many similarities to large-conductance Cl^- channels in other cell types, as discussed below.

Channel conductance

The conductance of this Cl^- channel in cultured trout gill pavement cells (372 pS) is very similar to that of large-conductance channels seen in other cell types bathed in solutions containing approximately 150 mmol l^{-1} Cl^-. Large-conductance

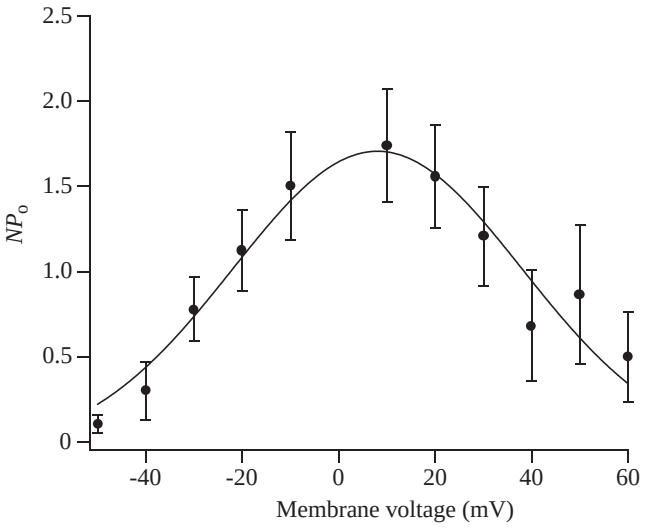

Fig. 7. Voltage-dependence of channel activity (NP_o) in inside-out patches. Currents were recorded from 20 consecutive sweeps at each voltage indicated between –50 mV and +60 mV. NP_o (mean ± 1 S.E.M.; N=6) was calculated from the mean currents for each patch divided by the corresponding single-channel current for the fully open state. NP_o was maximal near +10 mV.

Cl^- channels have been described in rat carotid body glomus cells (296 pS; Stea and Nurse, 1989), human T lymphocytes (365 pS; Schlichter et al., 1990), bovine aortic endothelial cells (382 pS; Olesen and Bundgaard, 1992), pulmonary alveolar epithelial cells (404 pS; Krouse et al., 1986) and a renal cortical collecting duct cell line (305 pS; Schweibert et al., 1994). The functions of large-conductance Cl^- channels are discussed below.

Channel selectivity

The ion selectivity of the large-conductance Cl^- channel in the pavement cells is similar to that seen in glomus cells (Stea and Nurse, 1989) and human T cells (Schlichter et al., 1990). Values of P_{SO_4}/P_{Cl} are 0.31, 0.49 and 0.57 in pavement cells, T cells and glomus cells, respectively. $P_{isethionate}/P_{Cl}$ is 0.53 and 0.56 in pavement cells and T cells, respectively, and P_{HCO_3}/P_{Cl} is 0.81, 0.56 and 0.71 in pavement cells, T cells and glomus cells, respectively. The relatively high permeability of HCO_3^- is of particular interest in the context of possible channel functions (discussed below).

Voltage-dependence of channel activity and voltage-dependent relaxation

The inverted U-shape of plots of channel activity *versus* membrane voltage is typical of maxi Cl^- channels studied to date. For example, P_o is low when the membrane potential is outside the range –40 to +40 mV in astrocytes and neuroblastoma cells (for a review, see Strange et al., 1996), but rises sharply between these voltages and is maximal at 0 to +10 mV. A common feature of large-conductance Cl^- channels is channel inactivation (or channel relaxation, as discussed below) in response to large polarizing voltages.

Large-conductance Cl^- channels in ciliary epithelial cells also inactivate when patches are polarized to voltages outside the range of approximately –40 mV to approximately +40 mV and activate at voltages within the range –20 mV to +20 mV. The inverted U-shaped activation curve in the steady state is in part a consequence of channel inactivation at the larger polarizations (Mitchell et al., 1997). In A6 cells (Nelson et al., 1984), bovine aortic endothelial cells (Olesen and Bundgaard, 1992) and colonic smooth muscle cells (Sun et al., 1993), polarization of maxi Cl^- channels to membrane voltages outside the range –20 mV to +20 mV also leads to a rapid inactivation of the channel.

The pattern of voltage-dependent inactivation in cultured pavement cells from gills of freshwater trout in this study is qualitatively similar to that seen in these other cell types. It is worth noting that Schlichter et al. (Schlichter et al., 1990) point out that maxi channel closure in human T1 lymphocytes in response to voltage jumps is best viewed not as classical inactivation, but rather as relaxation. A subsequent change to a membrane potential in a permissive voltage range (–20 to +20 mV) restores channel activity in lymphocytes. Schlichter et al. (Schlichter et al., 1990) proposed that the decrease in probability of finding the channel in the open state is consistent with the presence of two gates in series, one that closes at negative potentials and a second that closes at positive potentials. Both gates must be open for the channel to conduct. Importantly, neither closing event in large-conductance Cl^- channels is consistent with an inactivation gate, because channels closed by either a positive or negative voltage immediately re-opened when membrane voltage was returned to the permissive range between approximately –20 mV and approximately +20 mV. A similar restoration of current when membrane voltage is restored to 0 mV is seen in the pavement cell maxi Cl^- channel. The reduction in current seen in response to sustained polarization to voltages outside the range –20 mV to +20 mV is therefore best termed a voltage-dependent relaxation.

Sensitivity to Cl^- channel blockers

The pavement cell maxi channel was blocked by several drugs that effectively block maxi Cl^- channels in other cell types. A common feature of some of the drugs is the production of a flickery type of blockade during the early stages of drug exposure. The channels opened only in bursts of very rapid flickering between open and closed states, followed by permanent inactivation. This pattern was seen in the early stages of block of the channel by DIDS in the present study. Blockade by DIDS was irreversible, and poorly reversible or irreversible blockade has been seen in maxi Cl^- channels of the *Drosophila melanogaster* Malpighian tubule (O'Donnell et al., 1998), ciliary epithelial cells (Mitchell et al., 1997) and human T cell lymphocytes (Schlichter et al., 1990). In contrast, reversible blockade by DIDS has been found for cells of a human pancreatic cancer cell line (Becq et al., 1992). The related compound SITS reversibly blocks maxi Cl^- channels in ciliary epithelial cells (Mitchell et al., 1997), T cells (Schlichter et al., 1990), A6 cells (Nelson et al., 1984) and trout gill pavement cells (this study). Differences in the extent of reversibility of channel block by

disulphonic stilbene derivatives may be due to the formation of a covalent adduct between the drug and the channel protein through the isothiocyanate group (Cabantchik and Rothstein, 1972). Low levels (<45 μmol l^{-1}) of SITS irreversibly increase the number of transitions to subconductance states in endothelial maxi Cl^- channels (Vaca, 1999). In contrast, at concentrations above 45 μmol l^{-1}, the current amplitude of fully open and subconductance states is reversibly reduced (Vaca, 1999). It is worth noting that there also appears to be a reduction in open-channel amplitude when pavement cell maxi Cl^- channels recover from exposure to 1 mmol l^{-1} SITS (Fig. 12). Lastly, the channel blockade by the divalent cation Zn^{2+} at 1.0 mmol l^{-1} is reversible in human T cells (Schlichter et al., 1990) and partly reversible in pavement cells (this study).

Levels of total zinc (bound and unbound) measured in trout gills *in vivo* are approximately 0.5 mmol l^{-1} and may be elevated to approximately 1 mmol l^{-1} after exposure to sublethal zinc levels in the water (Hogstrand et al., 1995; Alsop et al., 1999), so our evidence for channel blockade by Zn^{2+} may have some environmental relevance. It will be of interest in future studies to determine the effects of other divalent cations on the pavement cell maxi channel, particularly in view of the importance of metal ions such as Zn^{2+}, Cu^{2+}, Ni^{2+} and Cd^{2+} as environmental pollutants. It must be noted that the inside of the channel was exposed to Zn^{2+} in our study, as in previous work on maxi Cl^- channels in human T cells (Schlichter et al., 1990), in which it is suggested that internal Zn^{2+} or Ni^{2+} plugs the channel (Schlichter et al., 1990).

Multiple subconductance states

A common characteristic of maxi Cl^- channels is the presence of multiple conductance levels (Krouse et al., 1986), which are thought to reflect coordinated openings of co-channels. Several findings in the present study suggest that the subconductance states seen in the pavement cells are due to the coordinated operation of co-channels. Direct transitions from the highest conductance state to a non-conducting state often occurred, suggesting extensive cooperativity of gating. All sublevels opened in the same range of membrane voltages as the highest conductance level, and all had linear *I*/*V* relationships in symmetrical solutions and shared the same reversal potential. Lastly, all substrates were completely blocked by Zn^{2+}, DIDS and diphenylamine carboxylate.

Channel density and estimates of Cl^- turnover time and flux

It is possible to estimate the channel density per cell from measurements of cell dimensions and the approximate tip

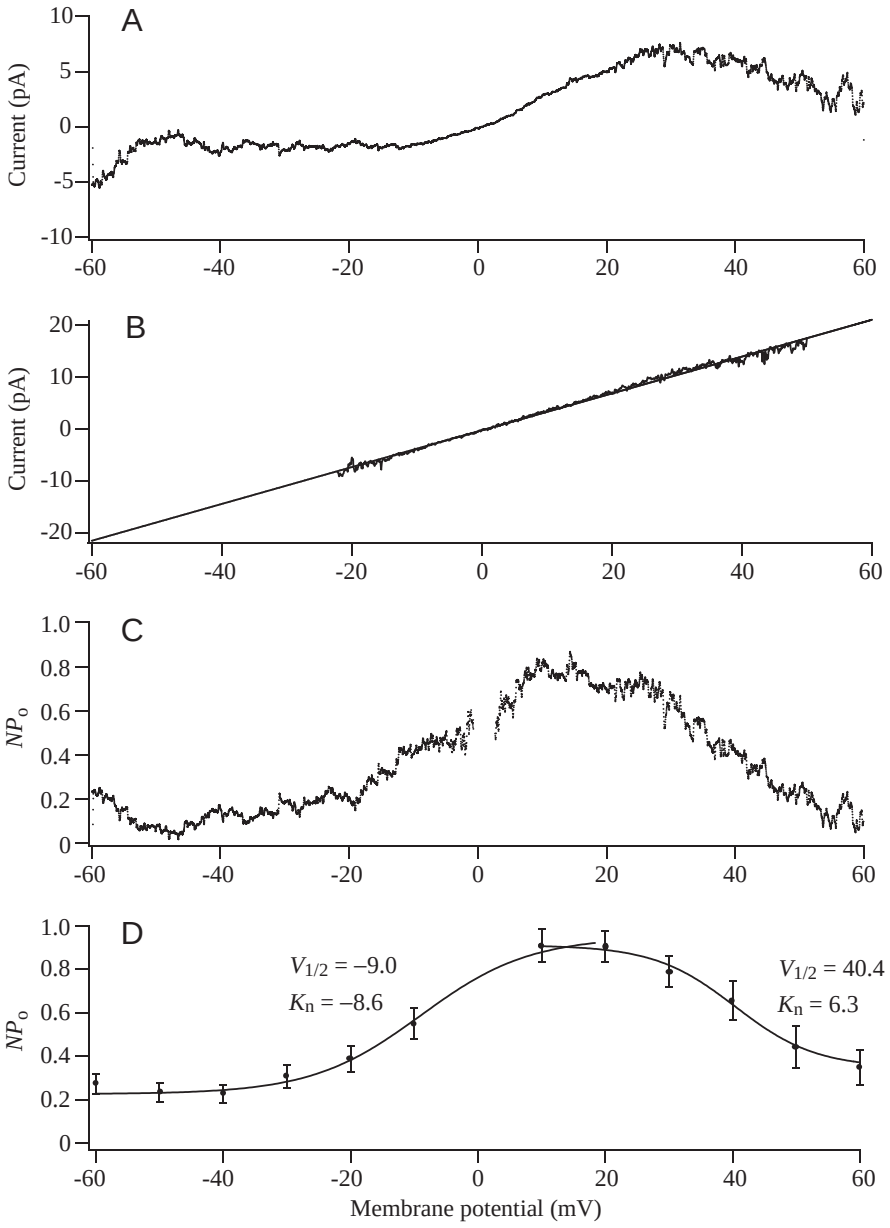

Fig. 8. Voltage-dependence of channel activity obtained from voltage ramps for inside-out patches. (A) Mean leak-corrected current (*I*) in an inside-out patch obtained when membrane potential was ramped from –60 to +60 mV. Each of 20 ramps of 1 s duration was followed by 200 ms at 0 mV. (B) Single-channel current (*i*) for the patch in A, obtained from conditional averaging as in Fig. 2. The solid line represents a linear fit to the data (r^2=0.997). (C) Channel activity (NP_o) for the patch in A and B calculated as *I*/*i*. (D) Mean channel activity for 19 inside-out patches. The curve was fitted as the sum of two Boltzmann equations of the form: $NP_o(V)=NP_{omax}/[1+e^{(V-V_{1/2})/K_n}]$, where $V_{1/2}$ is the voltage producing half-maximal channel activity and K_n is the slope factor corresponding to the voltage-sensitivity of activation. The fitted values (in mV) of $V_{1/2}$ and K_n for the left and right sides of the plot of NP_o *versus* membrane potential are indicated.

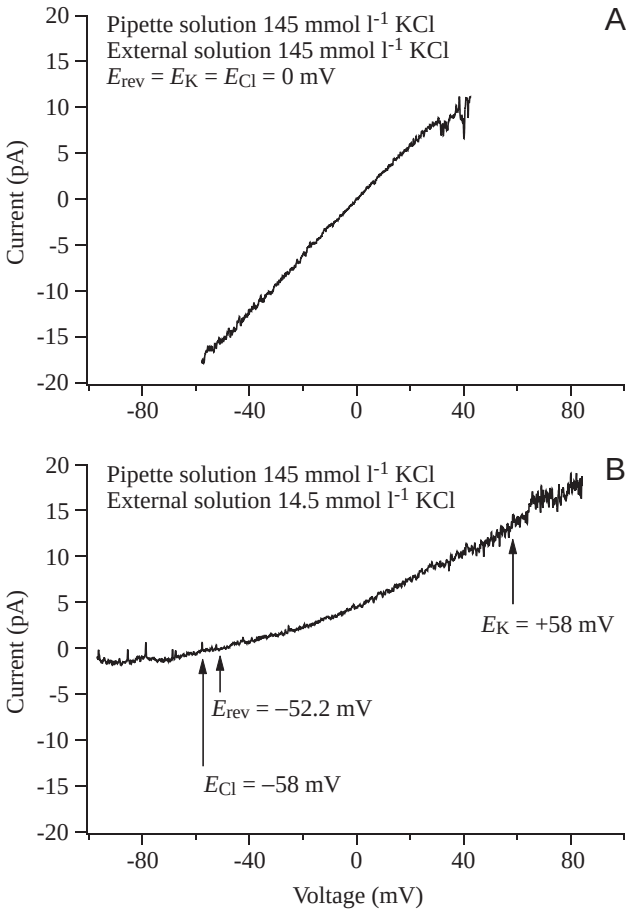

Fig. 9. The large-conductance channel is Cl^--selective. Single-channel currents for an inside-out patch in symmetrical salines (145 mmol l^{-1} KCl; A) and after a 10-fold reduction in KCl concentration in the external solution (B). Nernst equilibrium potentials for K^+ (E_K) and Cl^- (E_{Cl}) and the current reversal potential (E_{rev}) are indicated by the arrows. Currents were recorded in response to 20 voltage ramps of 1 s duration, and single-channel current was determined by conditional averaging as in Fig. 2.

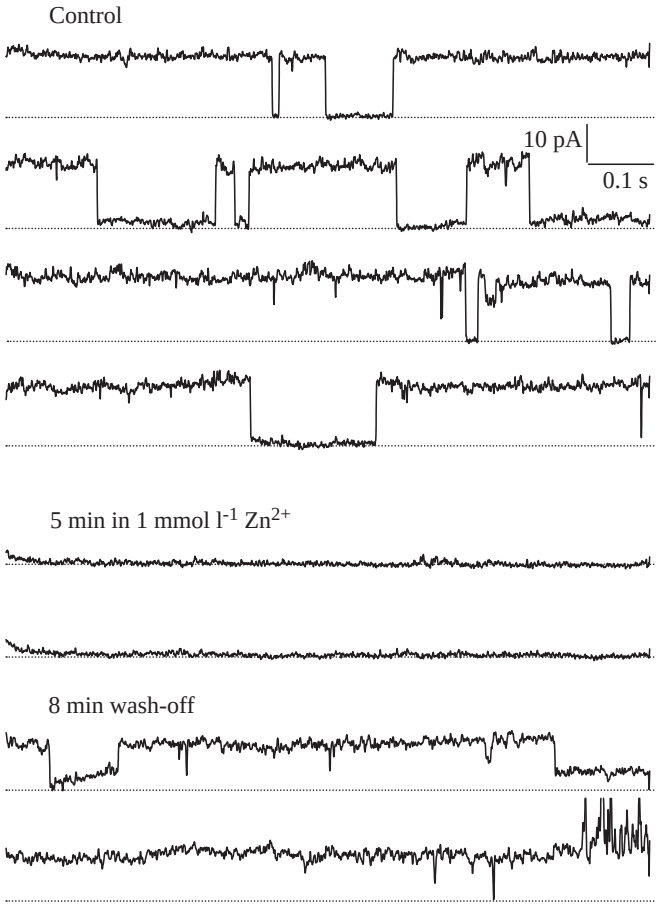

Fig. 10. Reversible block of the large-conductance Cl^- channel by Zn^{2+}. Current recordings for an inside-out channel are shown before (Control), 5 min after addition of 1 mmol l^{-1} Zn^{2+} to 150 NaCl saline (see Materials and methods) and 8 min after wash-off of Zn^{2+}. Membrane voltage was +20 mV for each recording.

diameter of the patch pipettes used in this study. The upward-facing area of each cell is 1970±74 μm^2 (mean ± S.E.M.) based on measurements of approximately 200 cells per field and five fields of view in light micrographs (C. M. Wood and S. P. Kelly, unpublished results). Given that 31 % of the patches contained maxi Cl^- channels, that there are 1.93 channels per patch and that the tip area for a pipette with an estimated diameter of 2 μm is 3.14 μm^2, there are approximately 375 maxi Cl^- channels per cell.

It is worth considering the impact that the opening of these channels could have on cellular Cl^- levels. For a conductance of 372 pS, if we assume a 10 mV difference between membrane potential and Cl^- equilibrium potential, then approximately 37 pA will flow through each channel, equivalent to (37 pA F^{-1}) 3.85×10^{-17} mol s^{-1} for one channel or 1.45×10^{-14} mol s^{-1} for all the channels in each cell. Cells are approximately 2 μm in depth, so cell volume is approximately 3.94×10^{-12} l. Using the cell Cl^- concentration of 49 mmol l^{-1} (Part and Bergstrom, 1995), the cell Cl^- content is 1.93×10^{-13} mol. The Cl^- flux through all the channels when fully open is thus sufficient to exchange the entire cell content of Cl^- in approximately 13 s ($=1.93\times10^{-13}$ mol/1.45×10^{-14} mol s^{-1}). Even if the channel open probability is as low as 0.2, a driving force of 10 mV would be sufficient to exchange the cell Cl^- content in approximately 1 min.

The calculations above indicate that the Cl^- flux for a 10 mV driving force would be approximately 1.45×10^{-14} mol s^{-1}/ 1970 μm^2=7.35×10^{-18} mol μm^{-2} s^{-1}, equivalent to 2644 nmol cm^{-2} h^{-1}. This value is approximately nine times the measured unidirectional flux of approximately 300 nmol cm^{-2} h^{-1} (Fletcher et al., 2000). Even if the open probability of the channels is reduced to 0.2, flux through maxi Cl^- channels exceeds measured values by approximately 1.7-fold. Thus, although the function of the maxi Cl^- channels in cultured pavement cells is not known, these calculations indicate that a role in transepithelial Cl^- transport is at least theoretically feasible.

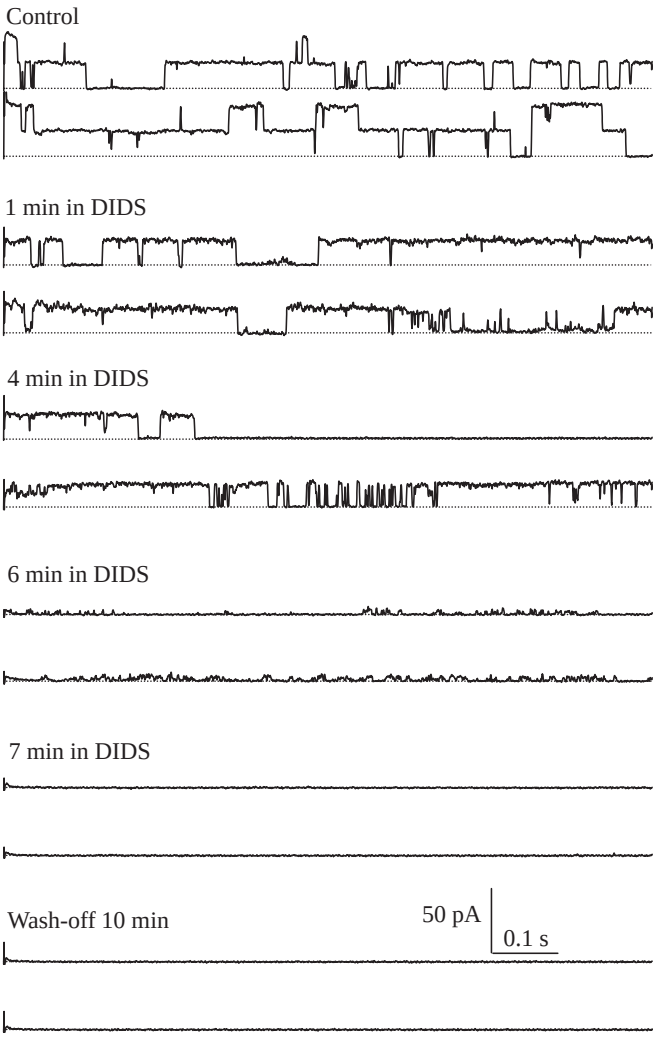

Fig. 11. Irreversible block of large-conductance Cl^- channels in an inside-out patch by 0.2 mmol l^{-1} DIDS. Membrane voltage was +20 mV for each recording. Recordings in the early stages of channel block (1–4 min after the addition of DIDS) show that the duration of channel opening was reduced but that there was no reduction in single-channel current.

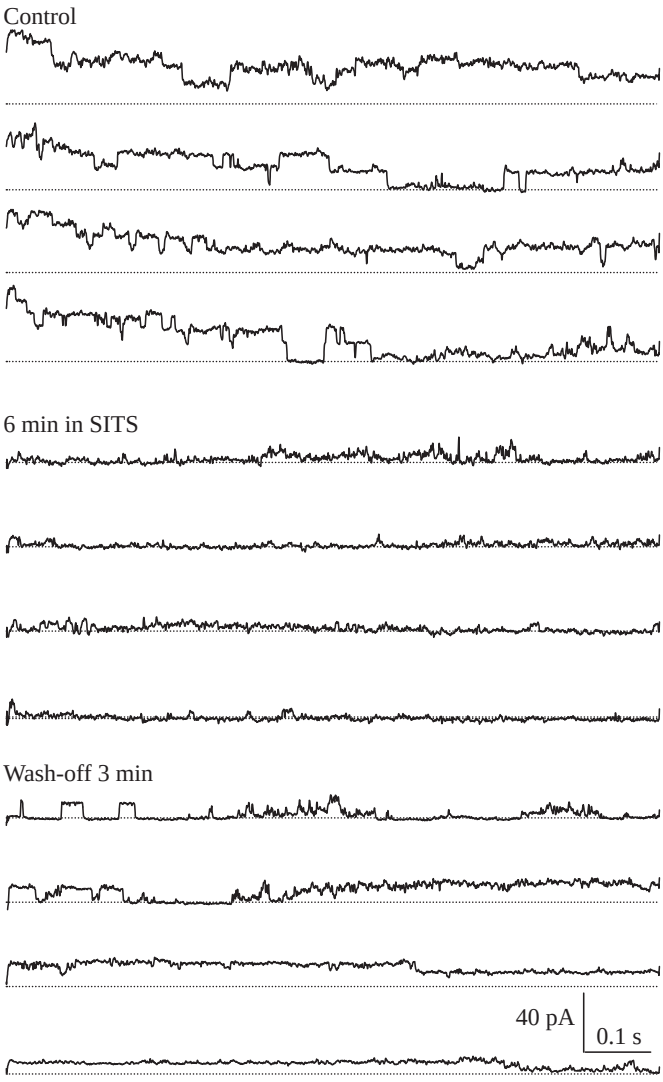

Fig. 12. Partly reversible block of large-conductance Cl^- channels in an inside-out patch by 1 mmol l^{-1} SITS. Membrane voltage was +20 mV for each recording.

Possible functions of large-conductance Cl^- channels in pavement cells

It is important to note that, although we patched the upward-facing surface of the cultured cells, which is known to exhibit the typical apical micro-ridges (Part and Bergstrom, 1995) seen *in vivo*, functional polarity is probably not maintained when cells are cultured in a medium resembling extracellular fluid. Under these conditions, it is probably inappropriate to use the terms apical and basolateral membrane. Therefore, we do not know on which functional surface the maxi Cl^- channels are normally expressed *in vivo*.

As noted in the Introduction, active Cl^- uptake by cultured pavement cells (Fletcher et al., 2000; Wood et al., 1998) does not fit any of our current models of freshwater ion transport. By the same token, active extrusion of Cl^- by cells in the cultured epithelium of the sea bass is not easily reconciled with accepted proposals for ion transport by the seawater gill (e.g. Zadunaisky, 1984). Nonetheless, two possible roles for maxi Cl^- channels in vectorial Cl^- transport come to mind. A Cl^- channel with a significant permeability to HCO_3^- could conceivably 'masquerade' as an apical Cl^-/HCO_3^- exchanger. Alternatively, a maxi Cl^- channel could function to move Cl^- from cell to blood after uptake across the apical surface.

In addition to their involvement in transepithelial Cl^- transport, Cl^- channels are thought to play important roles in cellular volume regulation (for a review, see Strange et al., 1996). Yet another function is suggested by the relatively high permeability of the channel to HCO_3^-. Efflux of HCO_3^- through the channel may contribute to the regulation of intracellular pH, preventing excessive increases in pH under alkalizing conditions. In this regard, Wood and Pärt (Wood and Pärt, 2000) found that recovery from intracellular alkalosis in cultured trout gill pavement cells was not dependent on Cl^-

and suggested that efflux of HCO_3^- through a specific channel could be the explanation.

It must be pointed out that pavement cells cultured in a medium resembling extracellular fluid may differentiate or de-differentiate so as to produce transport characteristics different from those seen *in vivo*. An important goal for subsequent studies is to make use of cultured pavement cells maintained on permeable inserts under asymmetrical conditions (tissue culture medium on the basolateral side and hypotonic medium on the apical side) so as to maintain cell polarity. Patch-clamp studies of pavement cells cultured under asymmetrical conditions can address questions concerning the presence, localization (apical *versus* basolateral) and functions of the maxi Cl^- channels described in this paper.

This study was supported by NSERC research and equipment grants to M.J.O., C.A.N. and C.M.W.

References

Al-Nakkash, L. and Hwang, T.-C. (1999). Activation of wild type and F508-CFTR by phosphodiesterase inhibitors through cAMP-dependent and -independent mechanisms. *Pflügers Arch.* **437**, 553–561.

Alsop, D. H., McGeer, J. C., McDonald, D. G. and Wood, C. M. (1999). Costs of chronic waterborne zinc exposure and the consequences of zinc accumulation on the gill/zinc interactions of rainbow trout in hard and soft water. *Env. Toxicol. Chem.* **18**, 1014–1025.

Avella, M. and Ehrenfeld, J. (1997). Fish gill respiratory cells in culture: a new model for Cl^--secreting epithelia. *J. Membr. Biol.* **156**, 87–97.

Barry, P. H. (1994). JPCalc, a software package for calculating liquid junction potential corrections in patch-clamp, intracellular, epithelial and bilayer measurements and for correcting junction potential measurements. *Neurosci. Meth.* **51**, 107–116.

Becq, F., Fanjui, M., Mahieu, I., Berger, Z., Gola, M. and Hollande, E. (1992). Anion channels in a human pancreatic cancer cell line (Capan-1) of ductal origin. *Pflügers Arch.* **420**, 46–53.

Cabantchik, Z. I. and Rothstein, A. (1972). The nature of the membrane sites controlling anion permeability of human red blood cells as determined by studies with disulfonic stilbene derivatives. *J. Membr. Biol.* **10**, 311–330.

Carl, A. and Sanders, K. M. (1990). Measurement of single channel open probability with voltage ramps. *J. Neurosci. Meth.* **33**, 157–163.

Duranton, C., Tauc, M., Avella, M. and Poujeol, P. (1997). Chloride channels in primary cultures of seawater fish (*Dicentrarchus labrax*) gill. *Am. J. Physiol.* **273**, C874–C882.

Egée, S., Mignen, O., Harvey, B. J. and Thomas, S. (1997). Chloride and non-selective cation channels in unstimulated trout red blood cells. *J. Physiol., Lond.* **511**, 213–224.

Fletcher, M., Kelly, S., Pärt, P., O'Donnell, M.J. and Wood, C.M. (2000). Transport and permeability properties of cultured branchial epithelia from freshwater rainbow trout: preparations with and without mitochondria-rich cells. *J. Exp. Biol.* **203**, 1523–1537.

Goss, G. G., Perry, S. F. and Laurent, P. L. (1995). Ultrastructural and morphometric studies on ion and acid–base transport processes in freshwater fish. In *Fish Physiology*, vol. 14, *Cellular and Molecular Approaches to Fish Ionic Regulation* (ed. C. M. Wood and T. J. Shuttleworth), pp. 257–284. San Diego, CA: Academic Press.

Hogstrand, C., Reid, S. C. and Wood, C. M. (1995). Ca^{2+} *versus* Zn^{2+} transport in the gills of freshwater rainbow trout and the cost of adaptation to waterborne Zn^{2+}. *J. Exp. Biol.* **198**, 337–348.

Kameyama, A., Yazawa, K., Kaibara, M., Ozono, K. and Kameyama, M. (1997). Run-down of the cardiac Ca^{2+} channel: characterization and restoration of channel activity by cytoplasmic factors. *Pflügers Arch.* **433**, 547–556.

Krouse, M. E., Schneider, G. T. and Gage, P. W. (1986). A large anion-selective channel has seven conductance levels. *Nature* **319**, 58–60.

Markwardt, F., Lohn, M., Bohm, T. and Klapperstuck, M. (1997). Purinoreceptor-operated cationic channels in human B lymphocytes. *J. Physiol., Lond.* **498**, 143–151.

Marshall, W. S., Bryson, S. E., Midelfart, A. and Hamilton, W. F. (1995). Low-conductance anion channel activated by cAMP in telost Cl^--secreting cells. *Am. J. Physiol.* **268**, R963–R969.

Mitchell, C. H., Wang, L. and Jacob, T. J. C. (1997). A large-conductance chloride channel in pigmented ciliary epithelial cells activated by GTPS. *J. Membr. Biol.* **158**, 167–175.

Nelson, D. J., Tang, J. M. and Palmer, L. G. (1984). Single-channel recordings of apical membrane chloride conductance in A6 epithelial cells. *J. Membr. Biol.* **80**, 81–89.

O'Donnell, M. J., Rheault, M. R., Davies, S. A., Rosay, P., Harvey, B. J., Maddrell, S. H. P., Kaiser, K. and Dow, J. A. T. (1998). Hormonally controlled chloride movement across *Drosophila* tubules is via channels in stellate cells. *Am. J. Physiol.* **43**, R1039–R1049.

Olesen, S.-P. and Bundgaard, M. (1992). Chloride-selective channels of large conductance in bovine aortic endothelial cells. *Acta Physiol. Scand.* **144**, 191–198.

Pärt P. and Bergstrom, M. E. (1995). Primary cultures of teleost branchial epithelial cells. In *Cellular and Molecular Approaches to Fish Ionic Regulation. Fish Physiology*, vol. 14 (ed. C. M. Wood and T. J. Shuttleworth), pp. 207–227. San Diego: Academic Press.

Pärt P. and Wood C. M. (1996). Na^+/H^+ exchange in cultured epithelial cells from fish gills. *J. Comp. Physiol*. B **166**, 37–45.

Perry, S. F. (1997). The chloride cell: structure and function in the gills of freshwater fishes. *Annu. Rev. Physiol*. **59**, 325–347

Schlichter, L. C., Grygorczyk, R., Pahapill, P. A. and Grygorczyk, C. (1990). A large, multiple-conductance chloride channel in normal human T lymphocytes. *Pflügers Arch.* **416**, 413–421.

Schweibert, E. M., Mills, J. W. and Stanton, B. A. (1994). Actin-based cytoskeleton regulates a chloride channel and cell volume in a renal cortical collecting duct cell line. *J. Biol. Chem.* **269**, 7081–7089.

Stea, A. and Nurse, C. A. (1989). Chloride channels in cultured glomus cells of the rat carotid body. *Am. J. Physiol*. **257**, C174–C181.

Strange, K., Emma, F. and Jackson, P. S. (1996). Cellular and molecular physiology of volume-sensitive anion channels. *Am. J. Physiol.* **270**, C711–C730.

Sullivan, G., Fryer, J. and Perry, S. (1995). Immunolocalization of proton pumps (H^+-ATPase) in pavement cells of rainbow trout gill. *J. Exp. Biol*. **198**, 2619–2629.

Sun, X. P., Supplisson, S. and Mayer, E. (1993). Chloride channels in myocytes from rabbit colon are regulated by a pertussis toxin-sensitive G protein. *Am. J. Physiol.* **264**, G774–G785.

Vaca, L. (1999). SITS blockade induces multiple subconductance states in a large conductance chloride channel. *J. Membr. Biol.* **169**, 65–73.

Wilson, J. M., Laurent, P., Tufts, B. L., Benos, D. J., Donowitz, M., Vogl, A. W. and Randall, D. J. (2000). NaCl uptake by the branchial epithelium in freshwater teleost fish: an immunological approach to ion-transport protein localization. *J. Exp. Biol.* **203**, 2279–2296.

Wood, C. M., Gilmour, K. M. and Pärt, P. (1998). Passive and active transport properties of a gill model, the cultured branchial epithelium of the freshwater rainbow trout (*Oncorhynchus mykiss*). *Comp. Biochem. Physiol.* **119**A, 87–96.

Wood, C. M. and Pärt P. (1997). Cultured branchial epithelia from freshwater fish gills. *J. Exp. Biol*. **200**, 1047–1059.

Wood, C.M. and Pärt, P. (2000). Intracellular pH regulation and buffer capacity in CO_2/HCO_3^--buffered media in cultured epithelial cells from rainbow trout gills. *J. Comp. Physiol*. B **170**, 175–184.

Zadunaisky, J. (1984). The chloride cell. In *Fish Physiology*, vol. 6, *Gills*, part B, *Ion and Water Transfer* (ed. W. S. Hoar and D. J. Randall), pp. 129–176. Orlando, FL: Academic Press.